Research Square

Preprints are preliminary reports that have not undergone peer review.
They should not be considered conclusive, used to inform clinical practice,
or referenced by the media as validated information.

# Rdii Dynamics in Coastal Sewer Systems: Influence of Downstream Boundary Conditions Based on Rtk Unit Hydrographs

**Paula Lidia Santana**
santana.paula28@gmail.com
Universidade Federal de Santa Catarina
**Jakcemara Caprario**
Universidade Federal de Santa Catarina
**Saman Belizário Broering**
Universidade Federal de Santa Catarina
**Priscila Batista Campos**
Universidade Federal de Santa Catarina
**Alexandra Rodrigues Finotti**
Universidade Federal de Santa Catarina

**Research Article**

**Keywords:** Coastal Sewer Systems, Flow Monitoring, Hydrological Modeling, Backwater Effect

**Posted Date:** August 5th, 2026

**DOI:** https://doi.org/10.21203/rs.3.rs-10491389/v1

**License:** This work is licensed under a Creative Commons Attribution 4.0 International License. Read Full License

**Additional Declarations:** No competing interests reported.

## Abstract

Stormwater flowing into sanitary sewers (RDII) creates serious urban management challenges, especially in coastal areas where water levels change frequently. This study assessed RDII patterns in the Lagoa da Conceição system (Florianópolis, Brazil) using the RTK unit hydrograph approach. Eight rain events at two pump stations (Ponte PS and Rendeiras PS) were reviewed using flow, rainfall, and tide/lake-level data. Key findings revealed that Ponte PS responded to events with a quicker and larger RDII flow, indicated by higher R coefficients and a greater vulnerability to stormwater entry. The timing and shape (T and K parameters, respectively) of the hydrograph at Ponte PS were significantly affected by lake level, confirming the presence of a backwater effect. In contrast, Rendeiras PS showed a slower, less pronounced response, with its RDII largely shaped by the sewer network design. Therefore, setting RTK values for coastal systems should include downstream effects rather than relying on generic figures. These findings highlight the need for targeted repairs and upgrades to enhance resilience against severe weather in coastal sanitation systems, clarifying where interventions are most needed.


## 1. INTRODUCTION

Urbanisation and more frequent extreme precipitation events have increased pressure on urban drainage and sanitary sewer infrastructure worldwide (Ferdowsi et al., 2024; Xie et al., 2025). Built-up area expansion leads to soil impermeabilization, which in turn alters the natural water cycle and increases surface runoff (Khan et al., 2025). This particularly affects sanitary sewer systems by encouraging unwanted stormwater entry—from illegal connections, infiltration, or structural flaws (Hrudka et al., 2020; Broering and Finotti, 2024). As a result, systems designed for steady domestic flow are subject to hydraulic overload during intense rainfall (Li et al., 2024).

Infiltration is groundwater entering sewers through defective joints, cracks, or porous pipes. Inflow results from stormwater entering via improper connections or wrongly connected drains (Tesfamariam et al., 2024; Zeydalinejad et al., 2024). Combined, these form Rainfall-Derived Infiltration and Inflow (RDII), responsible for sewer flow increases during rainfall. Depending on system age, infiltration and inflow can boost design capacity from 0.4 to 9 times the dry-weather flow (Bishop et al., 1987; Weiss et al., 2002; Bhaskar and Welty, 2012; Pangle et al., 2022). The literature documents the resulting increases in pumping and treatment flows, sewer overflows, and organic load dilution which impair biological treatment plants.

Rising wastewater volumes have multiple impacts. These include direct environmental harms such as water pollution, reduced dissolved oxygen levels, ecosystem damage, and public health risks. Greater flow also increases operational costs and shortens the lifespan of infrastructure, leading to frequent, costly repairs (Almeida and Jorge, 2025). Diluted effluent can cut BOD and TSS removal by 20–30%. This happens primarily because hydraulic retention time drops and biological processes become unstable, driving up treatment costs (Nan et al., 2024; Sowby and Jones, 2022).

A common way to analyse how drainage and sewer systems respond to rain is the unit hydrograph method. This tool, originally developed for watersheds, estimates changes in flow resulting from a specified amount of rainfall (Xu et al., 2025). When used in sewers, it helps quantify rain's impact on flow, estimate infiltration or inflow volumes, and identify vulnerable areas (Fadel and Dornelles, 2015). The method is also useful for detecting odd flow responses and calibrating models in urban sewer systems (Khatri et al., 2026).

Recently, many studies have used time series analysis and parametric models to fit unit hydrographs to observed data. Among these, the RTK method is prominent. It breaks the hydrological response into three components: fast, intermediate, and slow, each tied to particular inflow and infiltration mechanisms. 'R' is the fraction of rain that becomes sewer flow. 'T' measures time to peak flow. 'K' relates to how quickly the flow recedes and how long it lasts.

This approach allows robust estimation of rainfall-driven flows in many sewer systems, even where monitoring is incomplete (Perez et al., 2023). Applying RTK to real networks advances operational diagnostics. It uses high-frequency data and computational tools, making it easier to analyse and control urban stormwater flows (Yu et al., 2023).

Despite advances in analytical and computational methods, gaps remain in how RTK and similar approaches are used in working, separate sewer systems. This is especially true for coastal or sensitive environments. There, high groundwater, changing tides, and sandy or permeable soils promote constant infiltration and even reverse flow between aquifers and sewer pipes (Budd et al., 2020; Zeydalinejad et al., 2024). Tidal pressure swings can increase infiltration and disrupt the sewer's hydraulic state, making it harder to separate flow sources (Budd et al., 2020). Few studies have tracked rainfall and flows in such systems. This limits understanding and model accuracy (Zeydalinejad et al., 2024; Montoya-Coronado et al., 2024). Therefore, monitoring coastal systems is a top priority for better diagnostics and targeted control strategies.

From a wastewater system management perspective, understanding the hydraulic response of sewer networks to rainfall events is a key step in identifying structural and operational deficiencies. Quantifying rainfall-derived contributions enables distinguishing between actual domestic wastewater and the additional volume caused by infiltration and inflow (Bugajski et al., 2021).

This distinction is key for planning repairs, managing loss, and sizing treatment and pumping systems. It also supports Sustainable Development Goal 6 (SDG 6), which aims to achieve universal sanitation and improved water use (Dadebo et al., 2023). Evidence-based system management improves energy use and plant performance and supports sustainable operations, in line with national and international rules (Cardoso et al., 2021; Cassidy et al., 2023).

Standard models struggle with coastal boundary conditions. This study investigates how downstream hydraulic conditions shape RDII by analysing average unit hydrograph parameters using the RTK method. Two separate sewer subsystems in the Lagoa da Conceição basin, on Santa Catarina Island's east side (Brazil), were studied. This area is highly environmentally sensitive and has strong interactions between the urban and lagoon environments.

For analysis, rainfall events were picked from the monitored data. Each was used to calibrate unit hydrographs using the RTK method in Python. The study aims to describe the hydrological response and check how RTK parameters transfer in coastal areas with shifting boundaries.

## 2. METHODOLOGY

# 2.1. Study Area

The study area comprises two sanitary sewer subsystems, EE-B01 (Ponte) and EE-B02 (Rendeiras), located in the Lagoa da Conceição district, in the municipality of Florianópolis, southern Brazil (Fig. 1). This region is characterised by high environmental relevance and intense human occupation, with coexistence among consolidated urban areas, tourism infrastructure, and extensive preservation zones. The watershed is dominated by Lagoa da Conceição, a semi-enclosed lagoon connected to the Atlantic Ocean through the Barra Channel, with a total area of approximately 80 km², including a lagoon body of about 20 km². It is fed by watercourses such as the Capivaras, Vermelho, and João Gualberto rivers. The climate is humid subtropical with strong oceanic influence, characterised by high relative humidity, average annual precipitation of around 1,600 mm, and frequent winds and storms, including extratropical cyclones, especially during spring and summer. Precipitation is well distributed all over the year with monthly average of 150 mm.

From a geological and hydrogeological perspective, the region exhibits strong spatial heterogeneity, with granitic rock massifs interspersed with sedimentary plains of marine and lagoonal origin. Notable features include the Ingleses Aquifer, associated with fractured igneous rocks in the western portion of the basin, and the Campeche Aquifer, composed of highly permeable sandy deposits in the southern portion, both of which play a significant role in infiltration dynamics and groundwater storage. Soils range from sandy in flat areas to more developed profiles along hillside slopes, which are reflected in different vegetation patterns, including restinga formations and dense ombrophilous forests (Da Silva et al., 2024). Land use is characterised by the juxtaposition of environmentally sensitive areas (such as dunes and lagoon margins) and densely urbanised zones primarily dedicated to residential and tourism activities, posing significant challenges for the management of sanitation, urban drainage, and water resource quality.

The monitored subsystems exhibit significant structural contrasts that directly influence their hydrological responses. The Ponte PS system covers a watershed of approximately 0.72 km² and is served by a dense sewer network totalling 8,746 meters in length. In contrast, the Rendeiras PS system has a considerably larger contributing area of 3.52 km² but a shorter sewer network, totalling 5,841 meters. This configuration results in a much higher network density (pipe length per unit watershed area) in the Ponte subsystem

## 2.2. Hydrometeorological and Hydraulic Monitoring

The analysis of stormwater inflow and infiltration in the sanitary sewer system was based on a continuous hydrometeorological monitoring program designed to ensure high reliability and temporal resolution of precipitation and flow data. Monitoring was conducted over a two-year period, from September 2023 to September 2025, enabling capture of seasonal variability, extreme events, and short- and long-term hydraulic responses.

Rainfall data were obtained from the meteorological station operated by Epagri/CIRAM, located in the Itacorubi district (27°36’43,06” S; 48°28’29,84” W), approximately 5 km from the study area (Fig. 1). The station provides continuous precipitation records with hourly resolution, widely recognised for their consistency and reliability. Initially, the data were aggregated daily to identify discrete rainfall events and distinguish between dry and wet periods. Subsequently, hourly data were used to temporally align precipitation events with the hydraulic responses observed in the sewer system. This multiscale approach enabled capturing both high-intensity, short-duration events and prolonged moderate rainfall, which are essential for evaluating gradual infiltration processes in soils and pipelines.

Flow rates were monitored using continuous telemetry systems installed at both pumping stations: PS Ponte and PS Rendeiras (Fig. 01). Each station was equipped with Conaut electromagnetic flow meters, model WATERFLUX 3050W, properly calibrated and accompanied by metrological traceability certificates. The automated data acquisition and transmission system was configured to record instantaneous flow measurements at 1-minute intervals, resulting in continuous, consistent time series. The combination of high sampling frequency, rigorous instrument calibration, and uninterrupted telemetry operation ensured data representativeness and enabled the identification of daily and seasonal patterns, as well as transient responses associated with rainfall events.

Regarding downstream hydraulic conditions, tide-level data were analysed to assess the potential influence of sea-level fluctuations on the system's hydraulic behaviour, particularly in sections subject to controlled downstream conditions. These data were obtained from the tide gauge station operated by Epagri/CIRAM, identified as station 2951 – Florianópolis (South of the Island), located at coordinates 27.8161° S and 48.5639° W. The station provides continuous tide level records with a temporal resolution of 10 minutes.

Additionally, water level data from Lagoa da Conceição were incorporated to evaluate the influence of internal fluctuations on the hydraulic dynamics of the sanitary sewer system. These data were obtained from an independent

monitoring campaign conducted another research project developed in the region, which provided continuous records of lagoon water levels measured at a fixed point located at latitude 27°36'43.06"S and longitude 48°28'29.84"W. The measurements had a temporal resolution of 30 minutes, allowing for synchronised analysis with flow, precipitation, and tide data, as well as the investigation of the combined effects of internal lagoon levels and downstream conditions imposed by the tidal regime.

## 2.3. Pre-processing and Selection of Rainfall Events

The precipitation and flow time series were subjected to a systematic pre-processing procedure. Precipitation data were aggregated daily, enabling the selection of representative events. A minimum daily rainfall threshold of 10 mm was adopted to identify significant events, ensuring that only rainfall capable of generating relevant hydraulic responses was considered. In addition, a minimum antecedent dry period of seven days with non-significant precipitation (≤ 4 mm) was imposed, ensuring that the system was under predominantly dry conditions prior to the onset of each event. These criteria are consistent with established approaches in the literature on inflow and infiltration in sewer networks, ensuring comparability and robustness of the analysis (Lamin and Sezerino, 2012; Broering and Finotti, 2024). For each selected rainfall event, the corresponding flow time series was extracted, covering a 72-hour window before and after the event day, as recommended by Lamin and Sezerino (2012) and Broering and Finotti (2024). The time window was defined as starting at 00:00 (local time) on the day when daily precipitation was equal to or greater than 10 mm. Thus, the 72 antecedent hours correspond to the three full days preceding the event day, while the 72 subsequent hours correspond to the three full days following the event. This temporal standardisation allowed for consistent capture of baseflow conditions, the peak flow associated with rainfall, and the gradual return of the system to dry-weather flow, ensuring comparability among the analysed events.

Rainfall events were characterised based on precipitation records within the time window of each event. For each occurrence, the following parameters were calculated: total rainfall duration, cumulative precipitation, average intensity (defined as the ratio between total precipitation and event duration), and maximum observed intensity. These indicators were used to describe the severity, temporal structure, and potential for generating inflow and infiltration associated with each event.

The baseflow, representing the typical system flow under dry conditions, was estimated exclusively as the average of the hourly flow rates observed during the 72 hours preceding the onset of each rainfall event, a period during which no significant precipitation was recorded (Lamin and Sezerino, 2012; Broering and Finotti, 2024). Based on this constant baseflow, the inflow volume associated with precipitation was calculated through the temporal integration of the difference between the total observed flow and the baseflow, considering only the interval between the beginning of the rainfall event and the end of the system's hydraulic response. The integrated volume, expressed in cubic meters ($m^3$), represents the contribution of stormwater entering the sanitary sewer system through infiltration and inflow during each analysed event.

## 2.4. Application of the RTK Method

Although the RTK method is typically represented as the sum of three triangular unit hydrographs (associated with the fast, intermediate, and slow components of the hydrological response), preliminary analyses indicated a single dominant peak with relatively simple recession behaviour, without evidence of multiple hydrological processes.

Therefore, in this study, a single equivalent triangular hydrograph (simplified RTK) was used for each analysed event. This approach is particularly suitable for the Lagoa da Conceição sanitary sewer system, as it allows the representation of both short- and long-duration events and enables direct comparison between different subsystems, avoiding overparameterization during calibration while adequately capturing the predominant hydrological response.

In the simplified RTK method, each rainfall event was associated with a unit hydrograph defined by three fundamental parameters:

1. R (dimensionless), representing the efficiency of converting precipitation into inflow contribution to the system, defined as the ratio between the total RDII volume and the total precipitation volume over the drainage area;
2. T (h), corresponding to the time between the effective onset of flow increase (above dry-weather flow) and the occurrence of the hydrograph peak;
3. K (dimensionless), which controls the recession phase of the hydrograph, representing the ratio between the recession time and the time to peak.

The total RDII volume associated with each event was estimated through temporal integration of the excess flow relative to dry-weather flow. Initially, the average dry-weather flow was calculated as the mean flow observed over the three days (72 h) preceding the rainfall event, excluding periods influenced by rainfall.

Subsequently, for each event, the excess flow was defined as the difference between the observed flow and the dry-weather flow. The RDII volume was then obtained by integrating this excess over time. The parameter R was calculated as:

$$R = \frac{V_{RDII}}{V}$$

where $V_{RDII}$ is the total excess flow volume (m³), and Vrain is the total precipitation volume over the drainage area (m³), obtained from the cumulative rainfall of the event and the contributing area of each pumping station (Yu et al., 2023).

The time to peak (T) was determined as the interval between the initial moment when the excess flow becomes positive and the moment at which the maximum flow of the event occurs. The total duration (D) of the hydraulic event was defined as the interval between the beginning and the end of the period with positive excess flow. Based on this duration, the parameter K was calculated according to the following relationship:

$$K = \frac{D}{T} - 1$$

where D is the total duration of the hydraulic event (h). This formulation ensures geometric consistency of the triangular unit hydrograph, in which the total base equals T(1 + K).

The triangular unit hydrograph associated with each event was then defined by three characteristic points: the beginning of flow (0,0), the hydrograph peak (T, Qp), and the end of the recession (T(1 + K),0). The peak unit flow (Qp) was calculated based on volume conservation of the hydrograph, as follows:

$$Q_p = \frac{2R}{T\,(1+K)}$$

such that the area of the triangle is equal to the value of R.

For each pumping station and each selected rainfall event, the parameters R, T, and K were estimated individually, yielding a set of event-specific unit hydrographs. These hydrographs were subsequently superimposed and compared, allowing assessment of variability in hydraulic response across events and between subsystems.

# 2.5. Statistical Analysis and Interpretation of Results

The relationship between the simplified RTK method parameters and hydrometeorological variables was investigated through statistical correlation analysis and graphical representation. The associations were evaluated using the Spearman correlation coefficient (ρ), a nonparametric method that does not assume linearity or normality, making it particularly suitable for small sample sizes and for identifying monotonic relationships between variables (Vani et al., 2023).

All combinations between RTK parameters and explanatory variables associated with rainfall events and downstream hydraulic conditions were analysed. Among the pluviometric variables, the following were considered: event duration, total rainfall depth, average rainfall intensity, and maximum rainfall intensity. Additionally, the correlation analysis was extended to include variables representing downstream hydraulic control, namely the maximum tide level and the maximum water level in Lagoa da Conceição observed during the hydraulic response period of each event.

Correlations were evaluated individually for each pumping station, yielding 18 combinations of explanatory variables and RTK parameters for each analysed system. The results were graphically analysed using scatter plots, in which RTK parameters were plotted on the horizontal axis and hydrometeorological variables on the vertical axis.

In each diagram, in addition to the distribution of sample points, a trend line obtained through simple linear regression was included, along with the coefficient of determination ($R^2$) and the Spearman correlation coefficient (ρ). This approach allowed simultaneous evaluation of the strength, direction, and consistency of the observed associations without implying causality, and enabled an integrated interpretation of the influence of rainfall and downstream hydraulic conditions on the sanitary sewer system's response.

## 3. RESULTS

# 3.1. Characterisation of Rainfall Events

A total of eight rainfall events were selected that met the established criteria of minimum intensity and antecedent dry period (Table 1). The events occurred between October 2023 and July 2024 and exhibited substantial variability in duration, cumulative precipitation, rainfall intensity, and associated hydrodynamic conditions, as reflected in the maximum tide and lagoon levels recorded during each event. This combined variability allows for the representation of different interaction scenarios between pluviometric and hydrodynamic forcing typical of the study area. Although the monitoring period extended until September 2025, none of the events recorded in 2025 met the adopted selection criteria simultaneously and were therefore excluded from the analysis.

Table 1
Characteristics of the precipitation events selected for analysis, including start date, duration, accumulated precipitation, and average and maximum intensities.

| Event | Duration (h) | Average intensity ($mm.h^{-1}$) | Maximum intensity ($mm.h^{-1}$) | Precipitation (mm) | Maximum tide level (cm) | Maximum lagoon level (cm) |
|---|---|---|---|---|---|---|
| 28/10/23 | 33 | 1.79 | 7.60 | 59.20 | 99.70 | 99.97 |
| 01/01/24 | 13 | 1.05 | 5.80 | 13.60 | 104.30 | 102.78 |
| 25/02/24 | 5 | 6.88 | 24.60 | 34.40 | 48.70 | 87.67 |
| 05/04/24 | 6 | 3.07 | 13.60 | 18.40 | 119.20 | 89.02 |
| 25/04/24 | 9 | 2.22 | 9.00 | 20.00 | 126.00 | 103.17 |
| 17/06/24 | 6 | 1.70 | 3.00 | 10.20 | 68.60 | 50.37 |
| 06/07/24 | 34 | 3.06 | 9.60 | 104.20 | 131.80 | 127.75 |
| 29/07/24 | 4 | 2.90 | 5.40 | 11.60 | 72.60 | 91.30 |

The analysed events exhibited variable durations, ranging from 4 h to 34 h, with a predominance of short- to medium-duration events. Average rainfall intensities ranged from 1.05 $mm{\cdot}h^{-1}$ to 6.88 $mm{\cdot}h^{-1}$, indicating the occurrence of both moderate rainfall distributed the event and more concentrated, high-intensity episodes. Longer-duration events stand out, such as those recorded on October 28, 2023 (33 h) and July 6, 2024 (34 h), which were associated with intermediate average intensities (1.79 $mm{\cdot}h^{-1}$ and 3.06 $mm{\cdot}h^{-1}$, respectively). These characteristics are typical of persistent rainfall systems capable of promoting gradual accumulation of precipitation volumes and favouring inflow and infiltration processes.

Regarding maximum hourly intensities, a high degree of variability was observed among the events, with values ranging from 3.0 $mm{\cdot}h^{-1}$ to 24.6 $mm{\cdot}h^{-1}$. This pattern highlights the presence of intense rainfall peaks embedded within events of varying durations and average intensities. The event of February 25, 2024, stands out in this context, with the highest maximum hourly intensity (24.6 $mm{\cdot}h^{-1}$), the shortest duration (5 h), and the highest average intensity (6.88 $mm{\cdot}h^{-1}$). This indicates a strong temporal concentration of rainfall and a high potential for rapid, abrupt hydrological responses in the system.

It is also observed that events with similar cumulative rainfall volumes may exhibit markedly different temporal structures. The events of April 5, 2024 and April 25, 2024, with comparable total precipitation (18.4 mm and 20.0 mm, respectively), had durations of 6 h and 9 h, associated with average intensities of 3.07 $mm{\cdot}h^{-1}$ and 2.22 $mm{\cdot}h^{-1}$. In contrast, the most voluminous events, such as those recorded on October 28, 2023 and July 6, 2024, combined prolonged durations (33 h and 34 h) with high cumulative rainfall volumes (59.2 mm and 104.2 mm), as well as significant peak intensities. These characteristics define persistent rainfall episodes with intermittent intense peaks, which are potentially more critical from a hydrological perspective.

Regarding external hydrodynamic conditions, the events occurred under a wide range of maximum tide and lagoon levels. Maximum tide levels varied between 48.7 cm and 131.8 cm (with a historical average of 55 cm), while maximum lagoon levels ranged from 50.4 cm to 127.8 cm, with an average sampled level of 89.76 cm. Notably, the events of April 25, 2024 and July 6, 2024 were characterized by elevated tide levels (126.0 cm and 131.8 cm, respectively), coinciding with significant rainfall volumes or prolonged durations, thereby intensifying downstream flow

restrictions. In particular, the July 6, 2024, event simultaneously produced the highest cumulative rainfall (104.2 mm) and the highest lagoon level (127.75 cm), indicating a critical condition of an elevated hydraulic base level.

The combination of high-volume or high-intensity rainfall, prolonged durations, and elevated tide and lagoon levels suggests conditions favourable to the amplification of the system's hydrological responses. Increased downstream hydraulic levels may reduce drainage capacity, prolong recession times, and intensify temporary storage processes within the sanitary sewer network. Thus, the selected set of events adequately represents different interaction scenarios between pluviometric and hydrodynamic forcings, providing a consistent basis for the integrated analysis of flow-generation and propagation mechanisms in the studied system.

## 3.2. Observed Hydraulic Response at Pumping Stations

Figure 2 presents the flow time series observed at the Ponte PS and Rendeiras PS pumping stations for the eight selected rainfall events. For each event, measured flow rates, precipitation records, and tide and lagoon levels are displayed simultaneously, enabling an integrated evaluation of the sanitary sewer system's hydraulic response to rainfall and the downstream hydrodynamic conditions during each event.

In general, both subsystems exhibit a significant increase in flow during rainfall events, with a response clearly distinguishable from that under dry-weather conditions. In all analysed events, the rise in flow occurs after the onset of precipitation, indicating a predominantly delayed behaviour, characteristic of systems influenced by infiltration processes and progressive stormwater inflow.

The flow time series at Ponte PS shows greater variability amplitude, with more pronounced peaks and more abrupt responses in some events, especially during episodes with higher cumulative rainfall. In the events of October 28, 2023 and July 6, 2024, with totals exceeding 48 mm, a sustained increase in flow is observed over a longer period, followed by a gradual return to baseline conditions. However, the magnitude of the response does not appear to depend solely on the total rainfall volume, but also on the temporal distribution of precipitation. This behaviour may also be associated with the physical characteristics of the contributing area to Ponte PS, particularly steeper terrain and a higher sewer network density, which favour rapid surface runoff and may promote direct connections between stormwater drainage and the sewer system.

At Rendeiras PS, hydraulic responses are also clearly associated with rainfall events, but with lower relative magnitude and smoother flow peaks. The time series shows more regular variations, with gradual increases in flow and fewer abrupt peaks, suggesting structural and hydrological differences between the monitored subsystems.

In both cases, the persistence of elevated flow rates for extended periods after precipitation ends is noteworthy. This characteristic is particularly evident in longer-duration events, such as those in October 2023 and July 2024, where the return to baseflow occurs slowly and continuously. Such behaviour highlights the importance of delayed contribution processes, in contrast to the rapid and concentrated responses typical of direct inflow.

The inclusion of tide and lagoon level time series allows for a deeper interpretation of the observed hydraulic responses, highlighting the influence of downstream conditions on flow behaviour. In general, periods of elevated lagoon levels tend to coincide with sustained high flow rates, even after precipitation ends, indicating an increase in the hydraulic base level and a consequent restriction of drainage. This effect is particularly evident on July 6, 2024, when elevated and persistently high lagoon levels coincide with prolonged flow responses, suggesting the operation of backwater effects and temporary storage mechanisms within the system.

Tidal influence is observed as cyclical oscillations; however, only during the events of April 5, 2024 and July 6, 2024, is a possible tidal influence on the monitored flow series visually noticeable, contributing to the maintenance of elevated

flow levels over a longer period. At the July 6, 2024, event, it is also clear that lagoon levels increased during the rainfall event and have remained elevated over time. This supports the hypothesis of a potential influence of tidal elevation on the system, even if indirect and attenuated, given that Lagoa da Conceição is connected to the sea through the Barra da Lagoa Channel. The combination of prolonged rainfall, elevated lagoon levels, and high tide conditions may therefore delay drainage, extending recession times and sustaining flow rates above those in dry weather. This reinforces the integrated role of pluviometric and hydrodynamic forcing in shaping the sanitary sewer system's response.

Additionally, the time series reveal recurring daily patterns in flow rates, associated with wastewater generation and consumption under dry-weather conditions, on which the response to rainfall events is superimposed. During rainfall events, these patterns are partially masked by the abrupt increase in flow, especially during periods of higher rainfall intensity, suggesting direct inflow, possibly due to improper connections to the stormwater drainage system.

Table 2 presents the values of peak flow, average dry-weather flow, and the percentage increase in flow observed during rainfall events at the Ponte PS and Rendeiras PS pumping stations. These indicators allow assessment of the magnitude of the hydraulic response of the sanitary sewer system relative to normal operating conditions.

Table 2
Peak flows, dry weather flows, and flow increments observed during the analysed events.

| Event | Peak flow rate (L.s-1) | Peak flow rate (L.s-1) | Dry weather flow rate (L.s-1) | Dry weather flow rate (L.s-1) | Increase (%) | Increase (%) |
|---|---|---|---|---|---|---|
| | Ponte PS | Rendeiras PS | Ponte PS | Rendeiras PS | Ponte PS | Rendeiras PS |
| 28/10/23 | 27.30 | 16.72 | 10.73 | 6.56 | 154.43% | 154.88% |
| 01/01/24 | 13.14 | 9.95 | 12.55 | 9.88 | 4.70% | 0.71% |
| 25/02/24 | 29.85 | 15.45 | 10.47 | 7.27 | 185.10% | 112.52% |
| 05/04/24 | 24.23 | 16.21 | 10.15 | 5.72 | 138.72% | 183.39% |
| 25/04/24 | 27.20 | 14.51 | 10.80 | 6.21 | 151.85% | 133.66% |
| 17/06/24 | 22.70 | 13.73 | 10.41 | 5.33 | 118.06% | 157.60% |
| 06/07/24 | 25.53 | 19.07 | 9.87 | 5.59 | 158.66% | 241.14% |
| 29/07/24 | 26.02 | 13.53 | 10.50 | 6.66 | 147.81% | 103.15% |

The event of January 1, 2024, exhibited a distinct behaviour compared to the others, with a low hydraulic response at both pumping stations. Despite precipitation (13.6 mm), increases in flow relative to dry-weather conditions were minimal, reaching only 4.70% at Ponte PS and 0.71% at Rendeiras PS, indicating a negligible system response during this period. This behaviour may be related to the lowest average rainfall intensity (1.05 $mm \cdot h^{-1}$) among all selected events, highlighting the importance of this parameter in the analysis of inflow and infiltration processes within the system.

The largest increases in flow were observed in different events for each station. At Ponte PS, the event on February 25, 2024, stood out, with the highest peak flow (29.85 $L \cdot s^{-1}$) and the greatest relative increase over dry-weather flow (185.10%). At Rendeiras PS, the event on July 6, 2024, showed the highest percentage increase, rising 241.14% and reaching a peak flow of 19.07 $L \cdot s^{-1}$. Simultaneously, both stations exhibited similar responses during the October 28,

2023, event, with peak flows approximately 154% higher than in dry-weather conditions. This suggests the influence of additional factors (possibly related to the physical configuration of the sewer network and local topography) on the subsystems' sensitivity and hydraulic response.

The comparison between the two pumping stations reveals consistent differences in the magnitude of the hydraulic response. In general, Ponte PS exhibited higher peak flows than Rendeiras PS, highlighting the influence of sewer network length and density, given the significant difference between the contributing areas of the sub-basins. These differences may also be associated with the physical characteristics of the contributing areas, such as topography, soil type and land use, as well as the structural conditions of the pipelines and connections themselves.

## 3.3. RTK Curves

The analysis of normalised hydrographs and RTK parameters reveals important differences in the hydrological behaviour of the sewer network in the Ponte and Rendeiras subsystems, both in terms of temporal response and the volume associated with infiltration and inflow. Table 3 presents the RDII volumes and the estimated RTK parameters for each rainfall event at the pumping stations.

Table 3
Estimated RTK method parameters for precipitation events at the Ponte and Rendeiras pumping stations.

| System | Event | Duration (h) | Volume (m³) | R | T (h) | K |
|---|---|---|---|---|---|---|
| Ponte PS | 28/10/23 | 50.12 | 956.23 | 0.0223 | 29.53 | 0.697 |
| Ponte PS | 01/01/24 | 5.02 | 31.37 | 0.0032 | 4.15 | 0.209 |
| Ponte PS | 25/02/24 | 3.35 | 171.16 | 0.0069 | 0.23 | 13.382 |
| Ponte PS | 05/04/24 | 6.44 | 205.92 | 0.0155 | 4.83 | 0.334 |
| Ponte PS | 25/04/24 | 7.00 | 209.83 | 0.0145 | 4.07 | 0.722 |
| Ponte PS | 17/06/24 | 6.63 | 160.61 | 0.0217 | 3.23 | 1.052 |
| Ponte PS | 06/07/24 | 65.57 | 2,565.73 | 0.0340 | 32.30 | 1.030 |
| Ponte PS | 29/07/24 | 5.12 | 249.75 | 0.0297 | 1.42 | 2.615 |
| Rendeiras PS | 28/10/23 | 50.12 | 675.96 | 0.0032 | 39.72 | 0.262 |
| Rendeiras PS | 01/01/24 | 5.02 | 39.48 | 0.0008 | 4.62 | 0.086 |
| Rendeiras PS | 25/02/24 | 3.35 | 73.48 | 0.0006 | 0.80 | 3.183 |
| Rendeiras PS | 05/04/24 | 6.44 | 158.24 | 0.0024 | 4.82 | 0.337 |
| Rendeiras PS | 25/04/24 | 7.00 | 109.57 | 0.0016 | 3.89 | 0.797 |
| Rendeiras PS | 17/06/24 | 6.63 | 59.42 | 0.0017 | 5.76 | 0.152 |
| Rendeiras PS | 06/07/24 | 65.57 | 1,558.21 | 0.0043 | 45.62 | 0.437 |
| Rendeiras PS | 29/07/24 | 5.12 | 118.82 | 0.0029 | 2.33 | 1.192 |

At Ponte PS, the volumes associated with the events ranged from approximately 31 m³ to 2,566 m³, reflecting a highly variable network response to rainfall episodes. Short-duration events, such as January 1, 2024 and February 25, 2024, exhibited lower volumes, while longer events, such as October 28, 2023 and July 6, 2024, resulted in significantly

higher volumes. The parameter R mostly ranged from 1.4% to 3.3%, except for the two short-duration events, which showed conversions of precipitation volume into inflow and infiltration below 1%.

The parameter T, defined as the time to reach peak flow from the onset of the hydraulic response, was typically less than 5 h for most events, indicating that rapid responses were dominated by immediate inflow at Ponte PS. However, in atypical events with higher cumulative rainfall, T values exceeded 29 h, indicating that peak flow occurs later in prolonged responses, likely dominated by infiltration processes. Thus, the results suggest that T is strongly influenced by the duration of the response, reflecting both flow kinetics and the superposition of fast and slow contributions throughout the event. The parameter K exhibited wide variability (0.210 to 13.565), indicating distinct behaviours during the recession phase: short events showed more abrupt recessions, while longer events were associated with more persistent flows.

At Rendeiras PS, the estimated volumes ranged from approximately 39 $m^3$ to 1,558 $m^3$, also showing a clear dependence on event duration. As observed at Ponte PS, the largest volumes occurred during longer events (particularly on July 6, 2024), while short-duration events contributed little volume. Unlike Ponte PS, the parameter R values were consistently below 1%.

The response times T at Rendeiras PS were generally less than 6 h, except for extreme events, and were, in most cases, higher than those observed at Ponte PS for events of similar duration. Once again, a strong relationship between T and response duration is evident, with long events exhibiting delayed peaks exceeding 39 h, as in the cases of October 28, 2023 and July 6, 2024. This behaviour indicates a more attenuated system response, with greater influence from slow infiltration and storage processes. The parameter K ranged from 0.089 to 3.188, indicating that although recession is predominantly slow, the rate of return to dry-weather conditions varies across events, reflecting the interaction among event duration, accumulated volume, and the network's hydraulic characteristics.

Figure 3 presents the simplified RTK unit hydrographs for the analysed events at Ponte PS and Rendeiras PS, organised into two groups: typical-duration events (normal events) and long-duration events (special events) (October 28, 2023 and July 6, 2024). This separation was adopted to prevent the extended duration of these events from excessively stretching the time scale of the plots, which would visually flatten the hydrographs of the remaining events and hinder comparison of their shapes and peaks.

It is observed that, even among typical-duration events, Ponte PS exhibits earlier peak times, a response likely associated with the higher network density and length, as well as the topographic characteristics of its contributing sub-basin. In contrast, the hydrographs at Rendeiras PS display slower responses, with longer times to peak and, consequently, shorter recession periods, characteristic of networks with fewer branches and lower slopes. For long-duration events, both stations show more elongated hydrographs with delayed peaks, highlighting the greater influence of slower flow components. Even so, Ponte PS maintains more intense responses, while Rendeiras PS exhibits a more attenuated behaviour, consistent with its longer times to peak flow.

## 3.4. Relationship between Rainfall Characteristics, Downstream Boundary Conditions, and RTK Parameters

The dependence between rainfall event characteristics, tide and lagoon levels, and the parameters of the simplified RTK model is presented in the scatter plots shown in Fig. 4 (Ponte PS) and Fig. 5 (Rendeiras PS).

At the Ponte pumping station, the most consistent associations were observed between parameter T and rainfall duration and volume metrics. Rainfall duration showed a strong, statistically significant positive correlation with T (ρ =

0.874, $R^2$ = 0.965), as did total rainfall volume (ρ = 0.548, $R^2$ = 0.812), confirming that longer events shift the peak of the hydraulic response.

The parameter K showed a moderate positive correlation with average rainfall intensity (ρ = 0.452, $R^2$ = 0.864), suggesting that higher rainfall intensity may prolong the recession phase. In contrast, parameter R showed limited sensitivity to direct rainfall metrics, with correlation coefficients (ρ) ranging between 0.143 and 0.214.

Regarding downstream boundary conditions at Ponte PS, the maximum tide level had a stronger influence on time to peak (T) than the lagoon level, with a strong, significant correlation (ρ = 0.762). The lagoon level also exhibited a moderate to strong correlation with T (ρ = 0.619). These results indicate that external hydraulic control (particularly tidal influence) delays wave propagation within the network (backwater effect), with a reduced impact on volumetric magnitude (R) and recession behaviour (K).

At Rendeiras PS, a similar pattern of strong association between T and rainfall duration was observed (ρ = 0.778; $R^2$ = 0.955). Average and maximum rainfall intensities showed weak correlations with R (ρ = 0.048 and ρ = -0.143), reinforcing the independence of normalised volumetric magnitude from rainfall intensity. On the other hand, parameter K showed strong sensitivity to average rainfall intensity (ρ = 0.786; $R^2$ = 0.875), indicating that the recession phase is strongly influenced by rainfall event intensity in this subsystem.

Unlike Ponte PS, Rendeiras PS did not exhibit consistent patterns of external hydraulic control. Correlations between lagoon/tide levels and RTK parameters were predominantly weak to moderate and not statistically significant, suggesting that system variability is primarily driven by intrinsic rainfall characteristics and the structural properties of the local sewer network.

The pronounced difference in response magnitude between the subsystems can also be directly explained by their physical characteristics and network densities. While the Ponte PS system has a network of 8,746 m concentrated within an area of only 0.72 km² (resulting in a density of approximately 12.1 km/km²), the Rendeiras PS system features a more sparse network of 5,841 m distributed over a much larger area of 3.52 km² (density of 1.6 km/km²). This high density at Ponte PS increases the number of potential entry points for stormwater (such as pipe joints, manholes, and improper household connections) per unit area, which explains the significantly higher R values and the greater volumetric response observed in the hydrographs. In contrast, the larger contributing area of the Rendeiras subsystem, combined with a proportionally smaller network, favours flow attenuation and explains the smoother behaviour and longer response times (T) observed in this system.

Overall, the results indicate that the most significant correlations are concentrated in the relationships between rainfall duration/total volume and the parameter T, reinforcing that the time to peak of the unit hydrograph is strongly controlled by the temporal extent of the hydraulic response. In contrast, parameter R exhibited predominantly weak correlations, suggesting that the normalised volumetric magnitude of RDII does not depend solely on simple rainfall metrics but is likely influenced by the network's structural and operational characteristics, as well as the soil's hydrogeological and hydrodynamic storage properties. Parameter K showed more evident sensitivity to rainfall intensity in both systems. The differences observed between the two stations highlight the need for subsystem-specific analyses, as the hydraulic response to precipitation results from the interaction between rainfall characteristics, response duration, and the specific structural conditions of each network.

The analysis of correlations between hydrometeorological variables and RTK model parameters reveals significant differences between scenarios with and without the inclusion of long-duration, high-magnitude events (here, for comparison purposes, referred to as outliers), indicating that the interpretation of results is sensitive to the dataset composition. As shown in Table 4, excluding long events generally leads to substantial changes in both the magnitude

and, in some cases, the sign of the correlations, particularly for parameters T and K. This suggests that certain extreme events exert a significant influence on the observed statistical patterns.

For rainfall duration, for example, correlations with parameter T remain high at both monitoring points when all events are considered, indicating that longer events tend to shift the hydrograph peak to later times. However, after outliers are removed, the strength of these relationships decreases (especially at Rendeiras PS), with ρ and $R^2$ decreasing from 0.778 and 0.955 to 0.464 and 0.175, respectively. This may reflect either the loss of representative events or an apparent trend previously driven by high-magnitude events. The reduction in correlation strength highlights the need for further investigation using larger sample sizes and, potentially, distinguishing between long- and short-duration events to better represent the full hydrological and hydraulic behaviour of the system.

For parameter K, which represents the recession rate of the RDII hydrograph, the analysis shows high dispersion and notable changes in correlation behaviour between the two scenarios. At Ponte PS, for instance, the correlation with rainfall duration changes from $\rho = -0.575$ for the full dataset to $\rho = -0.841$ after removing outliers, suggesting increased sensitivity of this parameter to dataset structure. Similarly, at Rendeiras PS, significant changes are observed in the correlations between K and average rainfall intensity, which remain positive and relatively strong but differ in statistical significance across scenarios. These variations indicate that the recession phase of the hydrograph may be strongly influenced by high-magnitude rainfall events, which alter storage and flow dynamics within the sanitary sewer system.

Another relevant aspect is that, in some cases, excluding outliers reverses the sign of the correlations, particularly in relationships involving parameter R and pluviometric variables. This suggests that the system's hydrological behaviour may vary with rainfall volume or event intensity. This finding indicates that different rainfall regimes may activate distinct mechanisms of infiltration and inflow contribution, such as diffuse infiltration, improper connections, or temporary storage within the network. Thus, the combined analysis of both scenarios suggests that the system response is not homogeneous across events and may vary significantly with precipitation magnitude and duration.

Table 4
Correlations between hydrometeorological variables and RTK model parameters (R, T, and K) for the Ponte and Rendeiras pumping stations, considering scenarios with and without removal of long precipitation events.

| Variable | Parameter | Ponte PS | | | | Rendeiras PS | | | |
|---|---|---|---|---|---|---|---|---|---|
| | RTK | with outliers | | without outliers | | with outliers | | without outliers | |
| | | $R^2$ | Spearman ρ | $R^2$ | Spearman ρ | $R^2$ | Spearman ρ | $R^2$ | Spearman ρ |
| Rainfall duration | R | 0.194 | 0.18 | 0.448 | -0.638 | 0.474 | 0.419 | 0.267 | -0.406 |
| | T | 0.965 | 0.874 | 0.339 | 0.696 | 0.955 | 0.778 | 0.175 | 0.464 |
| | K | 0.099 | -0.575 | 0.183 | -0.841 | 0.136 | -0.503 | 0.23 | -0.754 |
| Mean rainfall intensity | R | 0.026 | 0.143 | 0.034 | 0.143 | 0.048 | 0.048 | 0.07 | 0.029 |
| | T | 0.046 | -0.143 | 0.563 | -0.371 | 0.037 | -0.286 | 0.696 | -0.543 |
| | K | 0.864 | 0.452 | 0.892 | 0.6 | 0.875 | 0.786 | 0.906 | 0.829 |
| Maximum rainfall intensity | R | 0.162 | -0.214 | 0.225 | -0.543 | 0.097 | -0.143 | 0.171 | -0.486 |
| | T | 0.026 | 0.143 | 0.229 | 0.029 | 0.026 | -0.143 | 0.487 | -0.486 |
| | K | 0.703 | 0.024 | 0.708 | 0.086 | 0.685 | 0.5 | 0.695 | 0.486 |
| Total rainfall depth | R | 0.272 | 0.214 | 0.284 | -0.6 | 0.498 | 0.333 | 0.292 | -0.6 |
| | T | 0.812 | 0.548 | 0.244 | -0.086 | 0.833 | 0.333 | 0.514 | -0.6 |
| | K | 0 | -0.048 | 0.729 | 0.143 | 0.002 | 0.286 | 0.737 | 0.543 |
| Maximum tide level | R | 0.041 | 0.214 | 0.025 | -0.086 | 0.231 | 0.429 | 0.044 | 0.257 |
| | T | 0.25 | 0.762 | 0.778 | 0.771 | 0.211 | 0.476 | 0.289 | 0.257 |
| | K | 0.494 | -0.571 | 0.53 | -0.714 | 0.394 | -0.143 | 0.403 | -0.314 |
| Maximum lagoon water level | R | 0.033 | 0.19 | 0.168 | -0.314 | 0.22 | 0.357 | 0.01 | -0.029 |
| | T | 0.347 | 0.619 | 0.016 | 0.371 | 0.32 | 0.31 | 0.128 | -0.257 |
| | K | 0.018 | -0.405 | 0 | -0.486 | 0.002 | -0.024 | 0.016 | -0.086 |

# 4. DISCUSSION

The results obtained allow for an integrated assessment of the hydrological and hydraulic response of the sanitary sewer systems at Ponte PS and Rendeiras PS under different rainfall events. High variability was observed among events, both in the volume of flow associated with rainfall-derived contributions and in temporal parameters, indicating that system response depends not only on total precipitation but also on the temporal distribution of rainfall and local hydraulic characteristics.

In both systems, parameter R ranged from 0.32% to 3.40% at Ponte PS and from 0.06% to 0.43% at Rendeiras PS. These values indicate that only a small fraction of precipitation is converted into rainfall-derived inflow and infiltration (RDII) within the analysed system. Such values fall within the ranges typically reported for urban systems, which generally range from 1% to 10% in systems with moderate infiltration (EPA, 2012; Rossman, 2015; Perez et al., 2023). Comparatively, the values obtained in this study lie at the lower end of the range observed internationally, such as

those reported by Yu et al. (2023) in South Korea (total R ranging from 0.85% to 2.39%), and are even more markedly below the values reported by Gheith (2010) in Columbus, USA (3.55% to 17.40%). This suggests that the analysed system (particularly at Rendeiras PS) has lower susceptibility to stormwater intrusion or benefits from better structural conditions.

The temporal parameters T and K also refuted the hypothesis of a static hydrological behaviour. The parameter T (time to peak) was within the commonly reported range of 2 to 12 hours (EPA, 2012; Khatri et al., 2026). In contrast, the parameter K (recession coefficient) exhibited wide dispersion, ranging from 0.210 to 13.565 at Ponte PS and from 0.089 to 3.188 at Rendeiras PS. In the study by Yu et al. (2023), K values ranged between 1.67 and 6.42, reflecting different recession rates associated with infiltration and storage mechanisms. This variability reinforces the idea that the recession phase is sensitive to the dynamics of each event rather than being governed solely by fixed network characteristics.

Statistical analyses help explain these variations. Spearman correlations indicated weak to moderate negative associations between rainfall intensity and parameter R, a pattern consistent with a hydraulic limitation effect: intense rainfall tends to favour direct surface runoff over gradual infiltration (Perez et al., 2023). On the other hand, parameter T showed a positive correlation with rainfall duration, indicating that prolonged events shift the peak of the hydraulic response to later times. Additionally, parameter K showed a moderate to strong correlation with rainfall intensity, suggesting that more intense events are associated with more persistent recession phases. This finding is consistent with Khatri et al. (2026), who found that the K3 component tended to increase with rainfall depth and peak intensity. This variability highlights that the efficiency of rainfall conversion into inflow is influenced by event-specific factors, such as antecedent soil moisture conditions, the degree of network saturation, and the presence of improper connections.

The event recorded on 25-Feb-24 illustrates a characteristic short-duration, high-intensity rainfall response. The corresponding unit hydrograph exhibits an early peak and rapid recession, indicating a predominance of fast inflow processes rather than delayed groundwater infiltration. Such behavior is commonly associated with direct stormwater connections, inflow through manhole covers, or rapid surface runoff entering the sewer system. From an operational perspective, these events resemble flash-flood conditions, in which large flows increase rapidly after rainfall onset. Early warning systems based on rainfall intensity thresholds could therefore support preventive actions, such as increasing the readiness of pumping stations and monitoring critical sewer reaches before peak flows.

In contrast, the long-duration events observed on 06-Jul-24 and 29-Jul-24 produced broad hydrographs with delayed peaks and extended recession limbs. These responses suggest that a significant portion of RDII originated from delayed infiltration pathways and temporary storage mechanisms within the catchment. Such events may not generate the highest instantaneous flows but can sustain elevated sewer flows for several days, increasing pumping energy consumption and reducing available storage capacity within the network.

The comparison among events further demonstrates that rainfall depth alone is insufficient to explain RDII generation. Events with comparable precipitation volumes produced markedly different hydrograph shapes, indicating that rainfall intensity, duration, antecedent moisture conditions, tidal influence, and hydraulic connectivity play a decisive role in determining sewer system response.

The identified hydrograph patterns provide useful information for utility operators. Events characterized by short response times and sharp peaks require rapid operational responses because pumping stations may experience sudden surges shortly after rainfall begins. Conversely, events associated with prolonged recession periods require longer monitoring windows since elevated flows may persist well after rainfall cessation. Therefore, classifying rainfall

events based on their expected RDII response may support risk-based operational planning, enabling utilities to optimize pump operations, schedule inspections, and prioritize maintenance activities.

The results reveal specific characteristics associated with the coastal context of the study area. Unlike non-coastal basins, where RDII response is primarily governed by interactions among soil, rainfall, and structural defects, coastal systems are subject to oscillations induced by tides. These variations alter the hydraulic gradient within the pipes, promoting cycles of infiltration and exfiltration and introducing additional signals in the flow, independent of rainfall. This factor increases the complexity of separating domestic and non-domestic flow components, suggesting that the system is sensitive not only to rainfall intensity but also to marine influence.

The analysis of the monitored events reveals three distinct RDII response patterns: rapid, intermediate, and delayed (Table 5). Rather than representing a continuum, these patterns reflect discrete hydrological behaviors governed by differences in response timing, peak development, and recession dynamics. This classification provides a structured framework to interpret event-to-event variability and reinforces that RDII generation cannot be adequately described by a single representative response. Instead, the results support the adoption of clustering-based approaches to define multiple RTK parameter sets, allowing for a more robust representation of the range of sewer system responses under varying rainfall and hydraulic conditions.

Table 5
Classification of RDII response patterns and their implications for sewer system operation and management.

| Response Pattern | Hydrograph Characteristics | Dominant RDII Mechanism | Representative Event(s) | Operational Implications |
|---|---|---|---|---|
| Rapid-response (Flash Flood Type) | Early peak, steep rising limb, short recession period, narrow hydrograph | Predominantly fast inflow from direct stormwater entry pathways | 25-Feb-24 | Requires rapid operational response due to sudden flow increases. Pumping stations should be monitored closely during high-intensity rainfall events, and rainfall-based warning thresholds may be useful for anticipating peak flows. |
| Intermediate-response | Moderate time to peak, balanced rising and recession limbs, intermediate hydrograph width | Combined influence of inflow and infiltration processes | 05-Apr-24<br>25-Apr-24<br>17-Jun-24 | Produces moderate flow increases that may affect system capacity. These events can be used as reference conditions for routine operational planning and model calibration. |
| Delayed-response (Storage/Infiltration Type) | Late peak, long recession period, broad hydrograph | Delayed infiltration, groundwater contribution, and catchment storage effects | 06-Jul-24<br>29-Jul-24 | May sustain elevated sewer flows for several days after rainfall ends, increasing pumping energy demand and reducing available storage capacity within the network. Long-term monitoring is recommended following these events. |

From a management perspective, identifying elevated R values provides guidance for directing inspections and rehabilitation efforts toward more susceptible areas. The variability of RTK parameters indicates that adopting a single

set of average values may be inadequate to represent all operational scenarios. Incorporating the derived unit hydrographs into hydrological-hydraulic models can contribute to more robust sizing of pumping and treatment facilities, reducing the risks of overloading, sewer overflows, and efficiency losses.

Some limitations should be considered. The number of events limits more robust inferential statistical analyses, and using a single rainfall station assumes spatial homogeneity that may not hold during short convective events. In addition, the RTK method treats infiltration and inflow as RDII in an integrated manner. Despite these limitations, the multi-event analysis identified robust hydraulic response patterns with potential applicability to similar urban systems.

In light of these findings, the results indicate the need to expand the dataset of analysed events and to possibly revise the criteria used to select rainfall events for RTK parameter calibration. The presence of substantial changes in correlations after removing long-duration events suggests that the current sample size may be insufficient to robustly capture the system's hydrological variability under different coastal rainfall conditions. In this context, the prior application of clustering techniques (e.g., cluster analysis) may be a useful strategy for identifying distinct hydrological response patterns associated with distinct rainfall regimes. Grouping events by pluviometric characteristics (e.g., low, medium, and high rainfall events) may improve the consistency of RDII dynamics representation and the calibration of RTK parameter sets that better reflect each hydrological regime. Thus, segmenting events by rainfall level may represent a relevant methodological advancement in system modelling, enabling a more accurate capture of variations in hydraulic response across different precipitation conditions.

# 5. CONCLUSIONS

This study evaluated the hydrological response of two sanitary sewer subsystems in Lagoa da Conceição to rainfall events and tidal level variations, using a simplified RTK method with a unit hydrograph to quantify rainfall-derived infiltration and inflow (RDII). The analysis of eight events between 2023 and 2024, integrating pluviometric and hydrodynamic variables, enabled the diagnosis of system sensitivity under different loading scenarios.

The results show that parameter R exhibits high variability, with higher magnitudes at Ponte PS than at Rendeiras PS, indicating the former is more susceptible to stormwater intrusion. Contrary to the assumption of parameter stability, temporal components proved dynamic: the time to peak (T) was strongly influenced by rainfall duration, while the recession coefficient (K) showed wide dispersion and sensitivity to rainfall intensity in both systems.

The comparison between the stations revealed distinct control mechanisms essential to operational management. Ponte PS exhibited more abrupt and volumetric responses, with evidence of external hydraulic control: elevated lagoon levels delayed the time to peak, suggesting a backwater effect. In contrast, Rendeiras PS showed a more attenuated response, largely independent of tidal boundary conditions, being primarily governed by intrinsic network characteristics and rainfall event properties.

In summary, the study confirms that the sewer system response extends beyond total precipitation volume, reflecting the complex interaction between event duration and the level of the receiving water body. These findings highlight the need for subsystem-specific calibration of RTK parameters, discouraging the use of generic values for basins with distinct hydrodynamic characteristics. A detailed understanding of these mechanisms provides critical support for hydraulic modelling and the planning of structural rehabilitation measures, being essential for sustainable sanitation management and climate adaptation in vulnerable coastal regions.

As future study perspectives, it is recommended to refine the criteria for selecting rainfall events, adapting them to the climatic specificities of each region and local precipitation characteristics. Thresholds for intensity and duration may vary significantly across hydrological regimes, thereby directly influencing the quality of model calibration. Additionally,

expanding the dataset to include more events will enable the application of clustering analyses based on statistical correlations. This approach will allow grouping events with similar hydrological responses, supporting the development of representative RTK unit hydrographs for different operational scenarios (such as low-intensity events under saturated soil conditions versus short-duration extreme events), thereby enhancing the accuracy and robustness of sanitary sewer system simulations.

# Declarations

**Acknowledgments**

This work has been supported by the Brazilian research agency CAPES. The authors are very grateful still to CASAN for supporting research activities.

**Funding details**

No funds, grants, or other support was received by organizations that may gain or lose financially through publication of this manuscript.

**Disclosure statement**

All authors certify that they have no affiliations with or involvement in any organization or entity with any financial interest or non-financial interest in the subject matter or materials discussed in this manuscript.

**Data availability statement**

The authors confirm that the data supporting the findings of this study are available within the article or its supplementary materials.

**Author contributions: CrediT**

**Paula Lidia Santana:** Conceptualization, Data Curation, Formal Analysis, Investigation, Methodology, Software, Visualization and Writing – Original Draft Preparation

**Jakcemara Caprario:** Methodology, Supervision, Validation and Writing – Review & Editing

**Saman Belizário Broering:** Investigation

**Priscila Batista de Campos:** Investigation

**Alexandra Rodrigues Finotti:** Supervision

**Declaration of generative AI and AI-assisted technologies in the manuscript preparation process**

During the preparation of this work, the authors used ChatGPT (OpenAI) for translation assistance and language refinement. After using this tool, the authors reviewed and edited the content as needed and take full responsibility for the content of the published article.

# References

1. Almeida, M., Brito, R., & Jorge, C. (2025). Inflows into wastewater and stormwater systems: Sources, causes, and assessment. Water. https://doi.org/10.3390/w17071082

2. Bhaskar, A. S., & Welty, C. (2012). Water balances along an urban-to-rural gradient of metropolitan Baltimore, 2001–2009. Environmental & Engineering Geoscience, 18(1), 37–50.
3. Bishop, W. J., Diemer, D. M., & Wallis, M. J. (1987). Regional infiltration/inflow study solves wet weather sewer problems. Journal of the Water Pollution Control Federation, 59(5), 289–293. http://www.jstor.org/stable/25043247
4. Broering, S. B., & Finotti, A. R. (2024). Estimation of infiltration and inflow due to precipitation in a sewage basin. Engenharia Sanitária e Ambiental, 29, e20230093. https://doi.org/10.1590/s1413-415220230093
5. Budd, E., Babcock, R., Spirandelli, D., Shen, S., & Fung, A. (2020). Sensitivity analysis of a groundwater infiltration model and sea-level rise applications for coastal sewers. Water. https://doi.org/10.3390/w12030923
6. Bugajski, P., Nowobilska-Majewska, E., & Majewski, M. (2021). The impact of atmospheric precipitation on wastewater volume flowing into the wastewater treatment plant in Nowy Targ (Poland) in terms of treatment costs. Energies. https://doi.org/10.3390/en14133806
7. Cardoso, B., Rodrigues, E., Gaspar, A., & Gomes, Á. (2021). Energy performance factors in wastewater treatment plants: A review. Journal of Cleaner Production. https://doi.org/10.1016/j.jclepro.2021.129107
8. Cassidy, J., Silva, T., Semião, N., Ramalho, P., Santos, A., Feliciano, J., Silva, C., & Rosa, M. (2023). Integrating reliability and energy efficiency assessments for pinpointing actionable strategies for enhanced performance of urban wastewater treatment plants. Sustainability. https://doi.org/10.3390/su151712965
9. Da Silva, R., Sakagami, Y., Haas, R., Farias, W., Rosa, G., Ramos, N., De Oliveira, G., & De Souza, D. (2024). Hydrometeorological monitoring of Lagoa da Conceição. Revista Contemporânea. https://doi.org/10.56083/rcv4n12-157
10. Dadebo, D., Obura, D., & Kimera, D. (2023). Hydraulic modeling and prediction of performance for a drinking water supply system towards the achievement of sustainable development goals (SDGs): A system case study from Uganda. Groundwater for Sustainable Development. https://doi.org/10.1016/j.gsd.2023.100951
11. Fadel, A. W., & Dornelles, F. (2015). Eficiência da interceptação de esgoto sanitário em rede pluvial na bacia do arroio Capivara-Porto Alegre/RS. Revista Brasileira de Recursos Hídricos, 20(4), 970–979.
12. Ferdowsi, A., Piadeh, F., Behzadian, K., Mousavi, S., & Ehteram, M. (2024). Urban water infrastructure: A critical review on climate change impacts and adaptation strategies. Urban Climate. https://doi.org/10.1016/j.uclim.2024.102132
13. Gheith, H. (2010). A stepped approach to generating a single set of RTK parameters for continuous calibration. Journal of Water Management Modeling. https://doi.org/10.14796/JWMM.R236-01
14. Hrudka, J., Marko, I., Šutúš, M., & Stanko, Š. (2020). Analysis of the efficiency of sewerage with illegal rainwater inflow. IOP Conference Series: Materials Science and Engineering, 867, 012010. https://doi.org/10.1088/1757-899X/867/1/012010
15. Khan, M., Keesstra, S., Słowik-Opoka, E., Klamerus-Iwan, A., & Liaqat, W. (2025). Determining the role of urban greenery in soil hydrology: A bibliometric analysis of nature-based solutions in urban ecosystem. Water. https://doi.org/10.3390/w17030322
16. Khatri, B., Wang, W., Pan, C., & Zhang, H. (2026). Assessment of rainfall-derived inflow and infiltration using smart sewer sensors and ensemble optimization. Journal of Water Process Engineering, 81, 109382.
17. Lamin, P. C., & Sezerino, P. H. (2012). Estimativa das infiltrações e afluxo devido à infiltração em rede coletora de esgoto. In Anais da 16ª Exposição de Experiências Municipais em Saneamento. ASSEMAE.
18. Li, W., Wang, Z., Zhou, J., Pang, Y., & Wang, H. (2024). Operation risk simulation and interaction impact of stormwater and sewage systems based on storm water management model. Water. https://doi.org/10.3390/w16070953

19. Montoya-Coronado, V., Tedoldi, D., Castebrunet, H., Molle, P., & Kouyi, G. (2024). Data-driven methodological approach for modeling rainfall-induced infiltration effects on combined sewer overflow in urban catchments. Journal of Hydrology. https://doi.org/10.1016/j.jhydrol.2024.130834
20. Nam, S., Lee, S., & Oh, J. (2024). Effect of rainfall-derived inflow and infiltration on dissolved organic matter in urban sanitary sewers using chemometric and machine learning approaches. Environmental Engineering Research. https://doi.org/10.4491/eer.2023.683
21. Pangle, L., Diem, J., Milligan, R., Adams, E., & Murray, A. (2022). Contextualizing inflow and infiltration within the streamflow regime of urban watersheds. Water Resources Research, 58. https://doi.org/10.1029/2021WR030406
22. Perez, G., Gomez-Velez, J., & Grant, S. (2023). The sanitary sewer unit hydrograph model: A comprehensive tool for wastewater flow modeling and inflow-infiltration simulations. Water Research, 249, 120997. https://doi.org/10.1016/j.watres.2023.120997
23. Rossman, L. A. (2015). Storm water management model user's manual version 5.1. U.S. Environmental Protection Agency.
24. Sowby, R., & Jones, D. (2022). A practical statistical method to differentiate inflow and infiltration in sanitary sewer systems. Journal of Environmental Engineering. https://doi.org/10.1061/(ASCE)EE.1943-7870.0001962
25. Tesfamariam, A., Heiderscheidt, E., Sunela, M., Pitkänen, A., Rantala, L., & Rossi, P. (2024). The estimation of infiltration and inflow in a sewage network by combining continuous monitoring of hydrological parameters, flow and temperature with stable isotopes. Water Research, 255, 121505. https://doi.org/10.1016/j.watres.2024.121505
26. US EPA. (2012). SSOAP toolbox enhancements and case study. Publication No. EPA/600/R-12/690.
27. Vani, P., Sahoo, B., Paul, J., Sahu, A., & Mohapatra, A. (2023). Trend analysis in gridded rainfall data using Mann-Kendall and Spearman's rho tests in Kesinga catchment of Mahanadi River Basin, India. Pure and Applied Geophysics, 180, 4339–4353. https://doi.org/10.1007/s00024-023-03379-8
28. Weiss, G., Brombach, H., & Haller, B. (2002). Infiltration and inflow in combined sewer systems: Long-term analysis. Water Science and Technology, 45(7), 11–19.
29. Xie, J., Qiang, W., Lin, Y., Huang, Y., Xu, K., Zheng, D., Chen, S., Pei, Y., & Fan, G. (2025). Enhancing urban drainage resilience through holistic stormwater regulation: A review. Water. https://doi.org/10.3390/w17101536
30. Xu, N., Sun, Y., Sun, Y., Sun, Z., & Geng, F. (2025). Prediction of flood processes based on general unit hydrograph. Water. https://doi.org/10.3390/w17020258
31. Yu, D., Jeon, J., Lee, J., & Kim, D. (2023). Development of an optimal RTK calculation program using genetic algorithm. Journal of the Korean Society of Hazard Mitigation. https://doi.org/10.9798/KOSHAM.2023.23.6.307
32. Zeydalinejad, N., Javadi, A., & Webber, J. (2024). Global perspectives on groundwater infiltration to sewer networks: A threat to urban sustainability. Water Research, 262, 122098. https://doi.org/10.1016/j.watres.2024.122098

## Figures

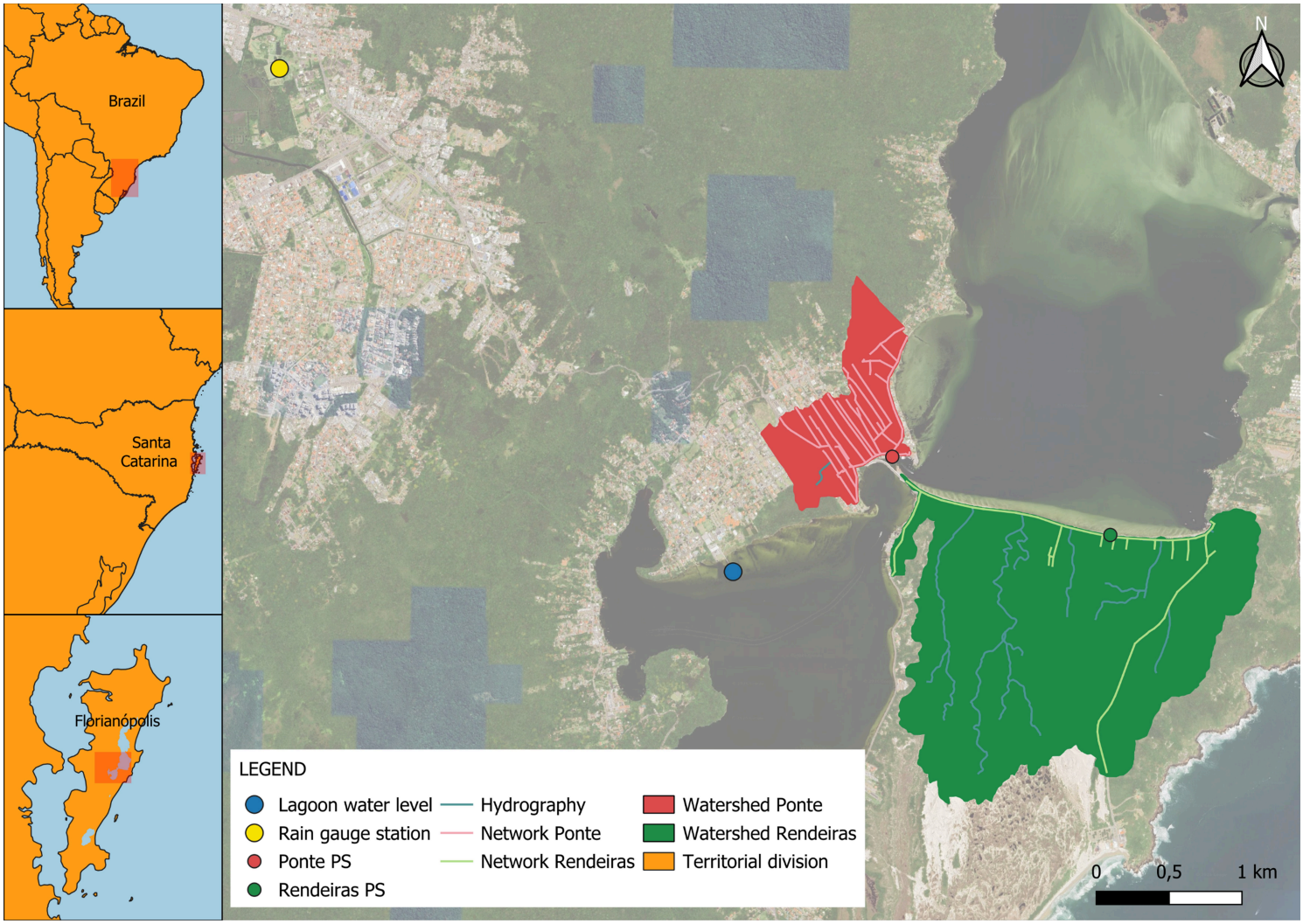
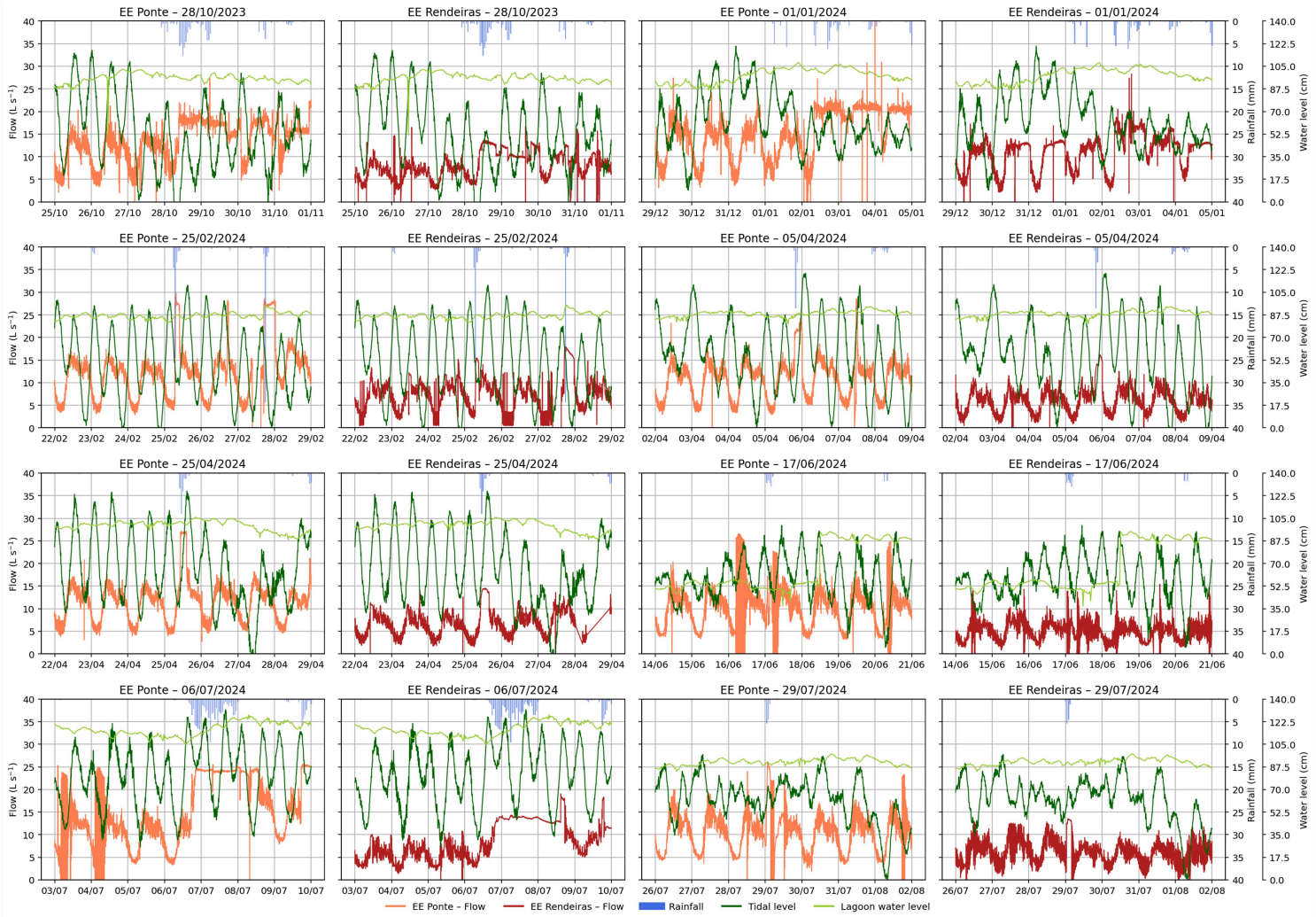


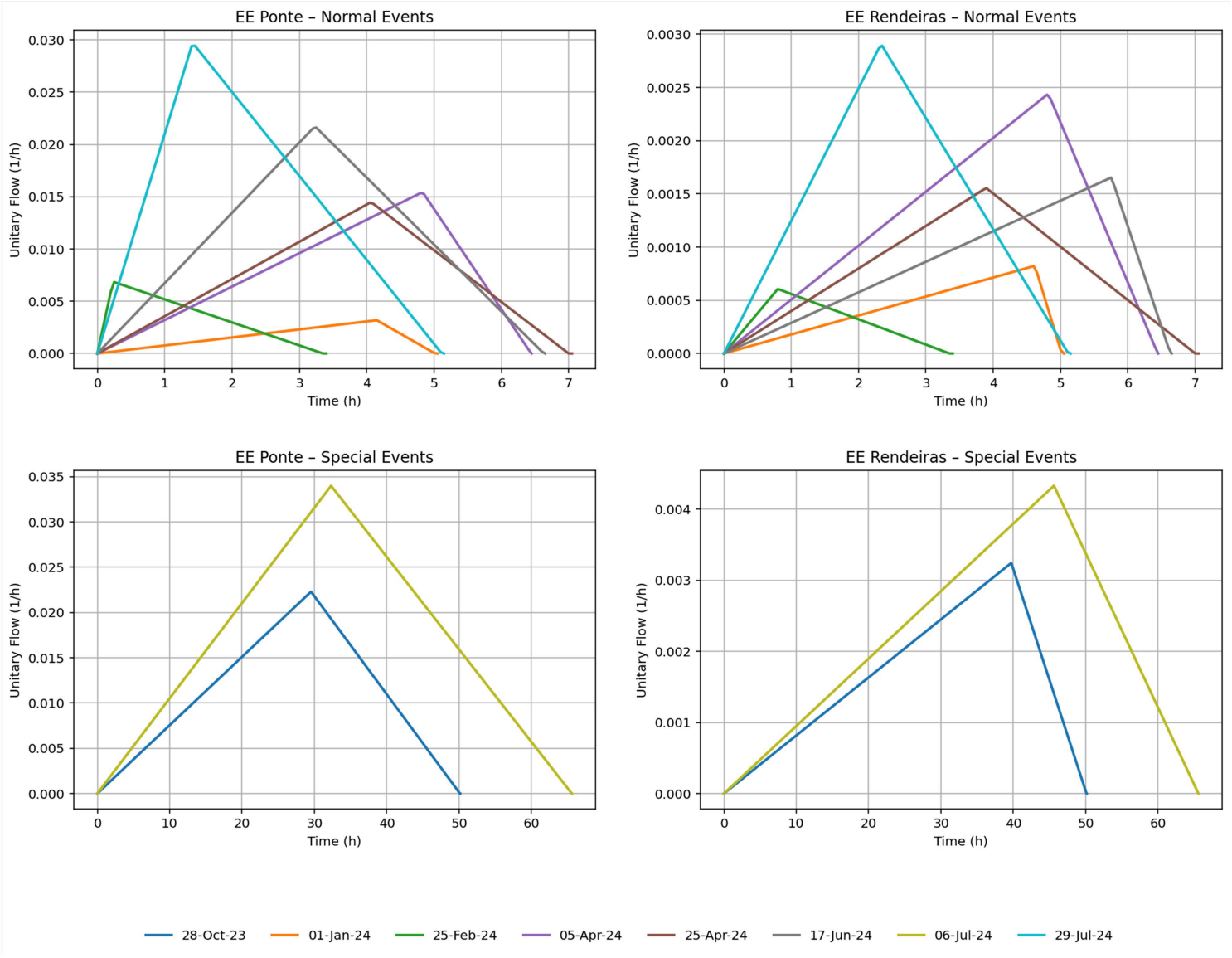

**Figure 1**

**Study area showing the Ponte and Rendereiras watersheds, sewer networks, and monitoring stations.**



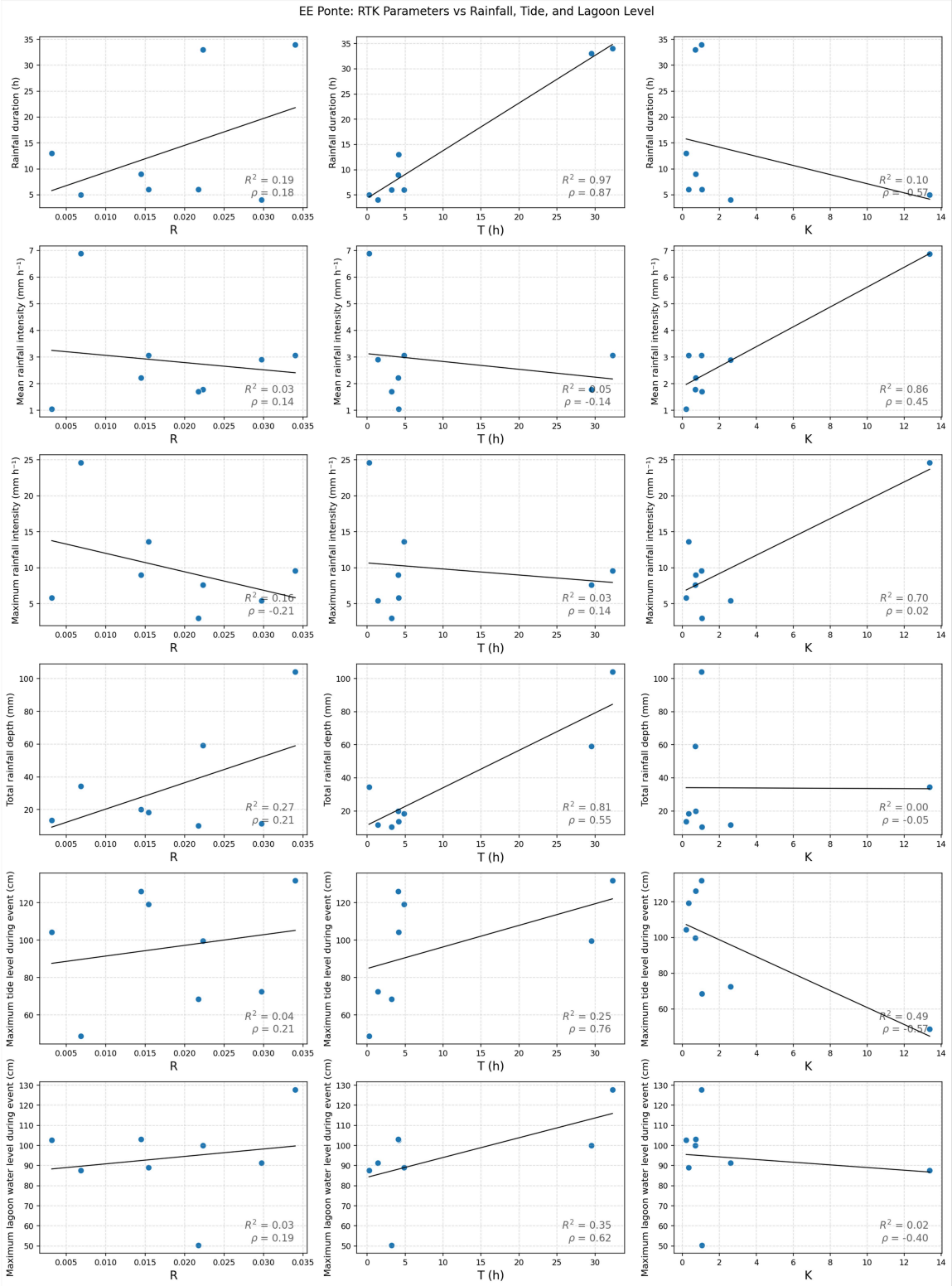

## Figure 2

**Flow rates observed at the Ponte PS and Rendeiras PS pumping stations during the analysed precipitation events, with the respective precipitation records, sea level, and lagoon level.**



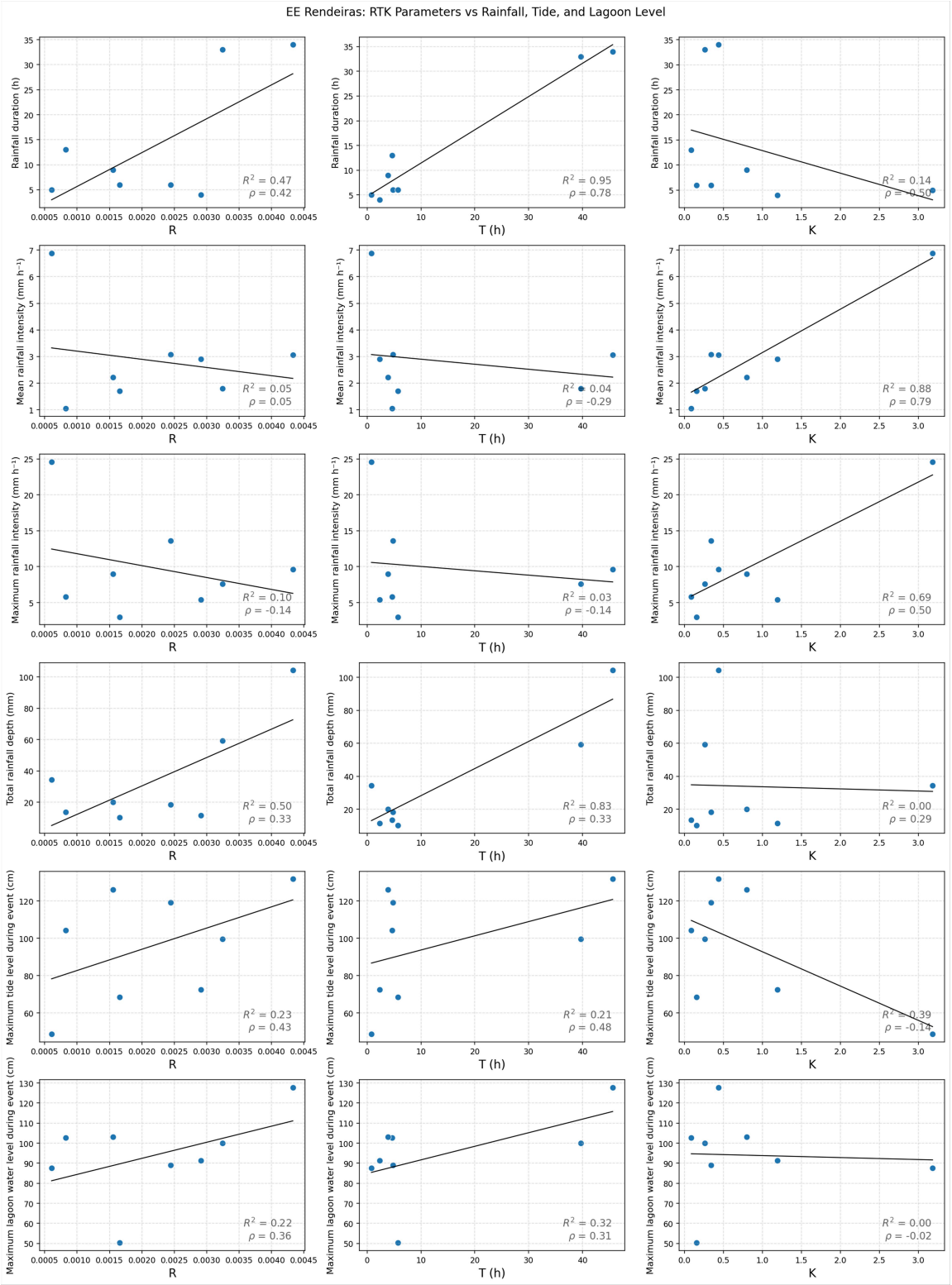

## Figure 3

**RTK unit hydrographs of the rainfall events analysed at the Ponte and Rendeiras pumping stations.**




## Figure 4

**Relationship between event characteristics and RTK parameters in the Ponte PS system.**




## Figure 5

**Relationship between event characteristics and RTK parameters in the Rendeiras PS system.**